

# Biometric classification system for dorsal finger creases utilizing multi-block circular shift combination local binary pattern

Imran Riaz<sup>1,2</sup>, Ahmad Nazri Ali<sup>1</sup>, Haidi Ibrahim<sup>1</sup>, Ilyas Ahmad Huqqani<sup>1</sup>

<sup>1</sup>School of Electrical and Electronic Engineering, Universiti Sains Malaysia, Penang, Malaysia

<sup>2</sup>Mirpur Institute of Technology, Mirpur University of Science and Technology, Mirpur, Pakistan

## Article Info

### Article history:

Received Apr 14, 2024

Revised Jul 10, 2024

Accepted Jul 17, 2024

### Keywords:

Biometrics

Classification

Dorsal finger crease

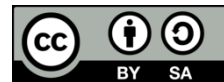
Feature extraction

Local binary pattern

## ABSTRACT

In recent years, there has been a growing interest in biometric recognition based on finger dorsal patterns, making it a significant area of research. This paper introduces a biometric classification system that utilizes dorsal finger middle creases. The viability of this trait is assessed through the implementation of a new method known as multi block circular shift combination local binary pattern (MBCSC-LBP). The MBCSC-LBP approach involves dividing the image into multiple blocks to enhance robustness and capture both local and global information, thereby extracting discriminative features. These features from each block are then concatenated to form a comprehensive feature vector. To evaluate the accuracy of the proposed MBCSC-LBP feature extractor, a support vector machine (SVM) with a linear kernel is utilized. The classification accuracy achieved by this method is 96.22% indicating a promising performance.

*This is an open access article under the [CC BY-SA](#) license.*



## Corresponding Author:

Ahmad Nazri Ali

School of Electrical and Electronic Engineering, Universiti Sains Malaysia

Nibong Tebal, Penang 14300, Malaysia

Email: nazriali@usm.my

## 1. INTRODUCTION

With the advancement and development of intelligent technologies, the demand for convenient and secure protection systems using biometric technology has received a widespread attention. Biometric systems are more reliable and effective as compared to the traditional identification systems such as postal index number (PIN) codes, verification documents, and tokens. Biometric technology refers to identifying and authenticating a user by utilizing the physiological or behavioral characteristics. The biometric-based systems have permeated the lives of human beings worldwide through a variety of applications, including secure financial transactions, identity verification, border control, forensic analysis, and smartphone authentication [1].

Hand-based modalities have a high recognition rate, typically utilize cost-effective image acquisition technology, small template sizes, and are user-friendly. In fact, different parts of the hand, such as fingerprint [2], finger vein [3], finger knuckle [4], hand geometry [5], and palm print [6], have been widely used as biometric traits for identification in existing systems. One of the earliest biometric techniques for verifying the user's identity is fingerprint recognition system. However, despite the successful progress, there are several concerns and limitations, including spoofing attacks, template reconstruction, and concerns over user privacy, since fingerprints are left on the surface of the acquisition device. Therefore, further efforts are required to explore and investigate alternative biometric features that can be employed in biometric systems more securely. Recently, dorsal finger crease is explored as an alternate biometric modality located on the back surface of the finger. Figure 1 illustrates the physiological traits of the dorsal finger surface, including the proximal knuckle or major knuckle, distal knuckle or minor knuckle, dorsal finger crease, and fingernail.

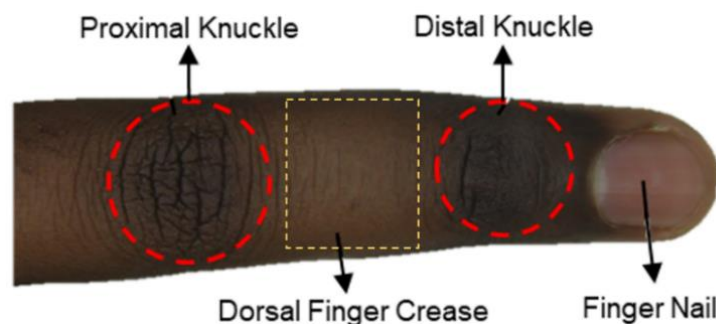


Figure 1. Dorsal finger surface anatomy with different biometric traits

In this paper, our aim is to further investigate the dorsal finger crease as an independent biometric identifier. The dorsal finger crease is located between the proximal knuckle and distal knuckle of the finger. Finger dorsal surface images contain lines pattern and much texture information, similar to other biometric images. However, to extract all those features, a robust extraction method is needed so that all the discriminant features can be extracted efficiently. The quality and complexity of the input image collection have a significant impact on the performance of each feature extraction approach. Local binary pattern (LBP), which is based on local features is robust to distortions, including rotation and illumination variations, and image scaling. The local binary pattern (LBP) and its variants have achieved promising results in numerous applications such as face recognition [7], finger vein biometrics [8], texture classification [9], plant-species recognition [10], and tumor classification [11]. The success of the LBP in these various applications inspired us to introduce an improved feature extraction method to extract key features with microstructure information, called multi-block circular shift combination local binary pattern (MBCSC-LBP).

The rest of the paper is organized as follows: section 2 presents the literature review of previous work in the field of finger biometrics and local binary pattern variants. Section 3 outlines the proposed research methodology. Section 4 presents and discusses the experimental results obtained, while section 5 concludes the study.

## 2. RELATED WORKS

In literature, numerous studies have explored the hand-based biometrics for identity recognition. Some have used hand-geometry [12] and palm-print [13] as distinct biometric identifiers. Other researchers have utilized finger-veins [14], which are features inside the human body, and finger-knuckles [15], located on the dorsal surface of the fingers. Petpon *et al.* [16] proposed a local line binary pattern (LLBP) for a face recognition system, which was later applied to a finger vein recognition system by Rosdi *et al.* [17]. The drawbacks of LLBP include feature extraction of only horizontal and vertical lines, without considering the entire image in various directions to utilize all available information. The finger-knuckle-print (FKP) was introduced as a biometric modality for the first time in 2009 by Zhang *et al.* [18] and utilized Gabor filters for feature extraction. Fingerprint recognition, which has been the most common and widely used biometric technology in numerous applications for many years [19]. However, studies have reported that individuals with skin diseases, exposure to chemical industries, and water immersion may fail to present clear fingerprints for identity verification [20]–[22]. Furthermore, previous literature studies have also highlighted the use of the inner surface of the hand, which includes fingerprints, finger veins, palm prints, palm veins, and inner finger knuckles, in biometric systems. The dorsal surface of the hand is less utilized, and FKP and fingernails are employed only in the personal identification systems.

To overcome the shortcomings of current biometric modalities and consider the significance of biometric systems in today's life, research on alternative biometric modalities for personal recognition is urgently needed. Dorsal finger crease (DFC) is an alternative and newly explored biometric modality [23]. The dorsal surface of the finger can be very helpful for biometric recognition since the features of finger back surface are stable remain unchanged and have long lifespan [24]. DFC is the skin region located between the major and minor knuckles of the dorsal finger surface. Surprisingly, the research community has not given more attention to this specific finger area. Moreover, to extract the prominent and useful features is a key step in biometric classification system. In this research, we investigate the use of the dorsal finger crease as an independent biometric modality using an improved feature extraction method called multi block circular shift combination local binary pattern (MBCSC-LBP).

### 3. METHOD

Figure 2 illustrates a complete overview of the proposed method for dorsal finger crease biometric classification system based on MBCSC-LBP. The proposed method is explained briefly in the subsequent subsections. Various tasks involved in our research work are covered in these subsections.

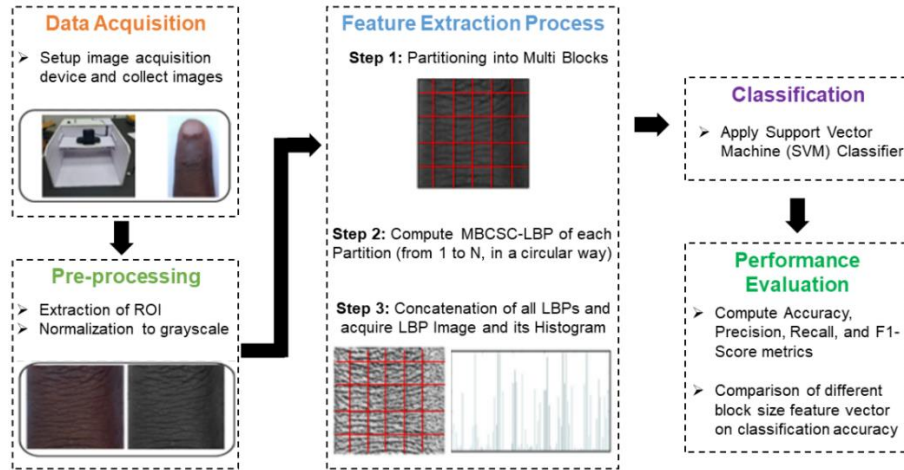


Figure 2. An overview of the proposed method

#### 3.1. Dataset acquisition

The dorsal finger images were captured by the apparatus shown in Figure 3, which consists of a Logitech Pro Webcam C920, a wooden case, and an LED light source. Using this acquisition apparatus, ten images of the left and right index fingers of each volunteer are captured. A total of 90 volunteers participated in collecting finger images, resulting in a total of 1,800 images being captured.

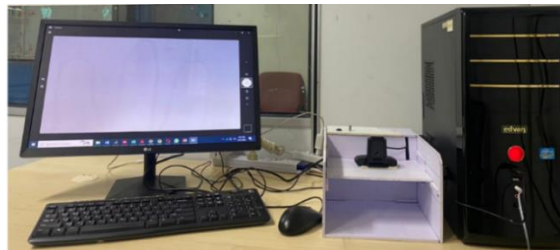


Figure 3. Image acquisition setup

#### 3.2. Pre-processing and ROI extraction

The dorsal finger images captured by the device contain unnecessary background information and need to be pre-processed to achieve higher classification accuracy. First, the desired two fingers are cropped and saved as right index and left index fingers in the database, separately. After that, region of interest extraction is performed, and images of pixel size 350×250 are extracted from two fingers of both hands. The sample ROI images are shown in Figure 4.



Figure 4. Sample ROI images of dorsal finger crease

### 3.3. Feature extraction

Feature extraction is crucial and plays a vital role in the performance of biometric recognition systems. Using extracted features instead of the complete data offers several key benefits: i) a better knowledge of the underlying features, ii) a reduction in dimensionality, iii) an enhanced ability for generalization, and iv) a decrease in computing costs. During the feature extraction process, important features are selected and improved for the given sample using predetermined algorithms.

The first step of MBCSC-LBP is to divide the DFC image into an appropriate number of sub-blocks. The local features of each sub-block of the DFC image differ and have a significant effect on the classification accuracy. This division of the image into sub-blocks is as follows: Let  $S$  be the DFC image, and then we divide  $S$  into an appropriate number of sub-blocks with a size of  $a \times b$  pixels. The partitioned image  $S$  can be represented as a  $p \times q$  matrix of all sub-blocks, as shown in (1).

$$S = \begin{pmatrix} S_{11} & S_{12} & \dots & S_{1q} \\ S_{21} & S_{22} & \dots & S_{2q} \\ \vdots & \vdots & \ddots & \vdots \\ S_{p1} & S_{p2} & \dots & S_{pq} \end{pmatrix} \quad (1)$$

Here the  $a, b \ll A, B$  and  $A \times B$  is the size of  $S$ . Also,  $S_{ij}$  is the  $(i, j)$  sub-block of the DFC image  $S$ .

The sub-blocks which are on the boundary of the image, may not be of same size and zero padding is performed to make the same size of all sub-blocks. The second step is to compute the circular shift combination LBP for each sub-block and obtain the local features using set of equations presented below.

CSCLBP<sub>0</sub>=(p<sub>0</sub>>p<sub>c</sub>), S(p<sub>1</sub>>p<sub>c</sub>), S(p<sub>2</sub>>p<sub>c</sub>), S(p<sub>3</sub>>p<sub>c</sub>), S(p<sub>4</sub>>p<sub>c</sub>), S(p<sub>5</sub>>p<sub>c</sub>), S(p<sub>6</sub>>p<sub>c</sub>), S(p<sub>7</sub>>p<sub>c</sub>);  
 CSCLBP<sub>1</sub>=S(p<sub>1</sub>>p<sub>c</sub>), S(p<sub>2</sub>>p<sub>c</sub>), S(p<sub>3</sub>>p<sub>c</sub>), S(p<sub>4</sub>>p<sub>c</sub>), S(p<sub>5</sub>>p<sub>c</sub>), S(p<sub>6</sub>>p<sub>c</sub>), S(p<sub>7</sub>>p<sub>c</sub>), S(p<sub>0</sub>>p<sub>c</sub>);  
 CSCLBP<sub>2</sub>=S(p<sub>2</sub>>p<sub>c</sub>), S(p<sub>3</sub>>p<sub>c</sub>), S(p<sub>4</sub>>p<sub>c</sub>), S(p<sub>5</sub>>p<sub>c</sub>), S(p<sub>6</sub>>p<sub>c</sub>), S(p<sub>7</sub>>p<sub>c</sub>), S(p<sub>0</sub>>p<sub>c</sub>), S(p<sub>1</sub>>p<sub>c</sub>);  
 CSCLBP<sub>3</sub>=S(p<sub>3</sub>>p<sub>c</sub>), S(p<sub>4</sub>>p<sub>c</sub>), S(p<sub>5</sub>>p<sub>c</sub>), S(p<sub>6</sub>>p<sub>c</sub>), S(p<sub>7</sub>>p<sub>c</sub>), S(p<sub>0</sub>>p<sub>c</sub>), S(p<sub>1</sub>>p<sub>c</sub>), S(p<sub>2</sub>>p<sub>c</sub>);  
 CSCLBP<sub>4</sub>=S(p<sub>4</sub>>p<sub>c</sub>), S(p<sub>5</sub>>p<sub>c</sub>), S(p<sub>6</sub>>p<sub>c</sub>), S(p<sub>7</sub>>p<sub>c</sub>), S(p<sub>0</sub>>p<sub>c</sub>), S(p<sub>1</sub>>p<sub>c</sub>), S(p<sub>2</sub>>p<sub>c</sub>), S(p<sub>3</sub>>p<sub>c</sub>);  
 CSCLBP<sub>5</sub>=S(p<sub>5</sub>>p<sub>c</sub>), S(p<sub>6</sub>>p<sub>c</sub>), S(p<sub>7</sub>>p<sub>c</sub>), S(p<sub>0</sub>>p<sub>c</sub>), S(p<sub>1</sub>>p<sub>c</sub>), S(p<sub>2</sub>>p<sub>c</sub>), S(p<sub>3</sub>>p<sub>c</sub>), S(p<sub>4</sub>>p<sub>c</sub>);  
 CSCLBP<sub>6</sub>=S(p<sub>6</sub>>p<sub>c</sub>), S(p<sub>7</sub>>p<sub>c</sub>), S(p<sub>0</sub>>p<sub>c</sub>), S(p<sub>1</sub>>p<sub>c</sub>), S(p<sub>2</sub>>p<sub>c</sub>), S(p<sub>3</sub>>p<sub>c</sub>), S(p<sub>4</sub>>p<sub>c</sub>), S(p<sub>5</sub>>p<sub>c</sub>);  
 CSCLBP<sub>7</sub>=S(p<sub>7</sub>>p<sub>c</sub>), S(p<sub>0</sub>>p<sub>c</sub>), S(p<sub>1</sub>>p<sub>c</sub>), S(p<sub>2</sub>>p<sub>c</sub>), S(p<sub>3</sub>>p<sub>c</sub>), S(p<sub>4</sub>>p<sub>c</sub>), S(p<sub>5</sub>>p<sub>c</sub>), S(p<sub>6</sub>>p<sub>c</sub>);

Combinations of CSCLBP

CSCLBP<sub>02</sub>=(CSCLBP<sub>0</sub>+CSCLBP<sub>2</sub>)/2; CSCLBP<sub>04</sub>=(CSCLBP<sub>0</sub>+CSCLBP<sub>4</sub>)/2;  
 CSCLBP<sub>06</sub>=(CSCLBP<sub>0</sub>+CSCLBP<sub>6</sub>)/2; CSCLBP<sub>24</sub>=(CSCLBP<sub>2</sub>+CSCLBP<sub>4</sub>)/2;  
 CSCLBP<sub>26</sub>=(CSCLBP<sub>2</sub>+CSCLBP<sub>6</sub>)/2; CSCLBP<sub>46</sub>=(CSCLBP<sub>4</sub>+CSCLBP<sub>6</sub>)/2;  
 CSCLBP<sub>024</sub>=(CSCLBP<sub>0</sub>+CSCLBP<sub>2</sub>+CSCLBP<sub>4</sub>)/3; CSCLBP<sub>046</sub>=(CSCLBP<sub>0</sub>+CSCLBP<sub>4</sub>+CSCLBP<sub>6</sub>)/3;  
 CSCLBP<sub>026</sub>=(CSCLBP<sub>0</sub>+CSCLBP<sub>2</sub>+CSCLBP<sub>6</sub>)/3; CSCLBP<sub>246</sub>=(CSCLBP<sub>2</sub>+CSCLBP<sub>4</sub>+CSCLBP<sub>6</sub>)/3;  
 CSCLBP<sub>0246</sub>=(CSCLBP<sub>0</sub>+CSCLBP<sub>2</sub>+CSCLBP<sub>4</sub>+CSCLBP<sub>6</sub>)/4;  
 CSCLBP<sub>13</sub>=(CSCLBP<sub>1</sub>+CSCLBP<sub>3</sub>)/2; CSCLBP<sub>15</sub>=(CSCLBP<sub>1</sub>+CSCLBP<sub>5</sub>)/2;  
 CSCLBP<sub>17</sub>=(CSCLBP<sub>1</sub>+CSCLBP<sub>7</sub>)/2; CSCLBP<sub>35</sub>=(CSCLBP<sub>3</sub>+CSCLBP<sub>5</sub>)/2;  
 CSCLBP<sub>37</sub>=(CSCLBP<sub>3</sub>+CSCLBP<sub>7</sub>)/2; CSCLBP<sub>57</sub>=(CSCLBP<sub>5</sub>+CSCLBP<sub>7</sub>)/2;  
 CSCLBP<sub>135</sub>=(CSCLBP<sub>1</sub>+CSCLBP<sub>3</sub>+CSCLBP<sub>5</sub>)/3; CSCLBP<sub>137</sub>=(CSCLBP<sub>1</sub>+CSCLBP<sub>3</sub>+CSCLBP<sub>7</sub>)/3;  
 CSCLBP<sub>157</sub>=(CSCLBP<sub>1</sub>+CSCLBP<sub>5</sub>+CSCLBP<sub>7</sub>)/3; CSCLBP<sub>357</sub>=(CSCLBP<sub>3</sub>+CSCLBP<sub>5</sub>+CSCLBP<sub>7</sub>)/3;  
 CSCLBP<sub>1357</sub>=(CSCLBP<sub>1</sub>+CSCLBP<sub>3</sub>+CSCLBP<sub>5</sub>+CSCLBP<sub>7</sub>)/4;

After computing CSC-LBP, concatenate these LBP features of each sub-block to obtain a complete MBCSCLBP feature vector. The entire framework for computing MBCSC-LBP is illustrated in Figure 5. The selection of the sub-block size has a significant impact on the final classification accuracy and is discussed in detail in the results section.

### 3.4. Performance evaluation

The classification process was performed using a support vector machine (SVM) with the feature vectors obtained by MBCSC-LBP for different block sizes. The training classification processes run 10 times, and the average of these 10 experiments is reported in the results. In this study, accuracy, precision, recall, and F1-score are performance metrics that have been computed to evaluate the proposed method. Most of the time, the system's classification performance is evaluated primarily on accuracy. The ability of the classification model to identify the actual number of positive cases out of all positive predictions is termed as precision. It is defined as the ratio of true positives to the sum of true positives and false positives. The

model's ability to correctly identify true positives is measured using recall. The harmonic mean of recall and precision is known as the F1-score. These four metrics are defined as in (2)-(5).

$$Accuracy = \frac{t_p + t_n}{t_p + t_n + f_p + f_n} \quad (2)$$

$$Precision = \frac{t_p}{t_p + f_p} \quad (3)$$

$$Recall = \frac{t_p}{t_p + f_n} \quad (4)$$

$$F1 - Score = \frac{2t_p}{2t_p + f_p + f_n} \quad (5)$$

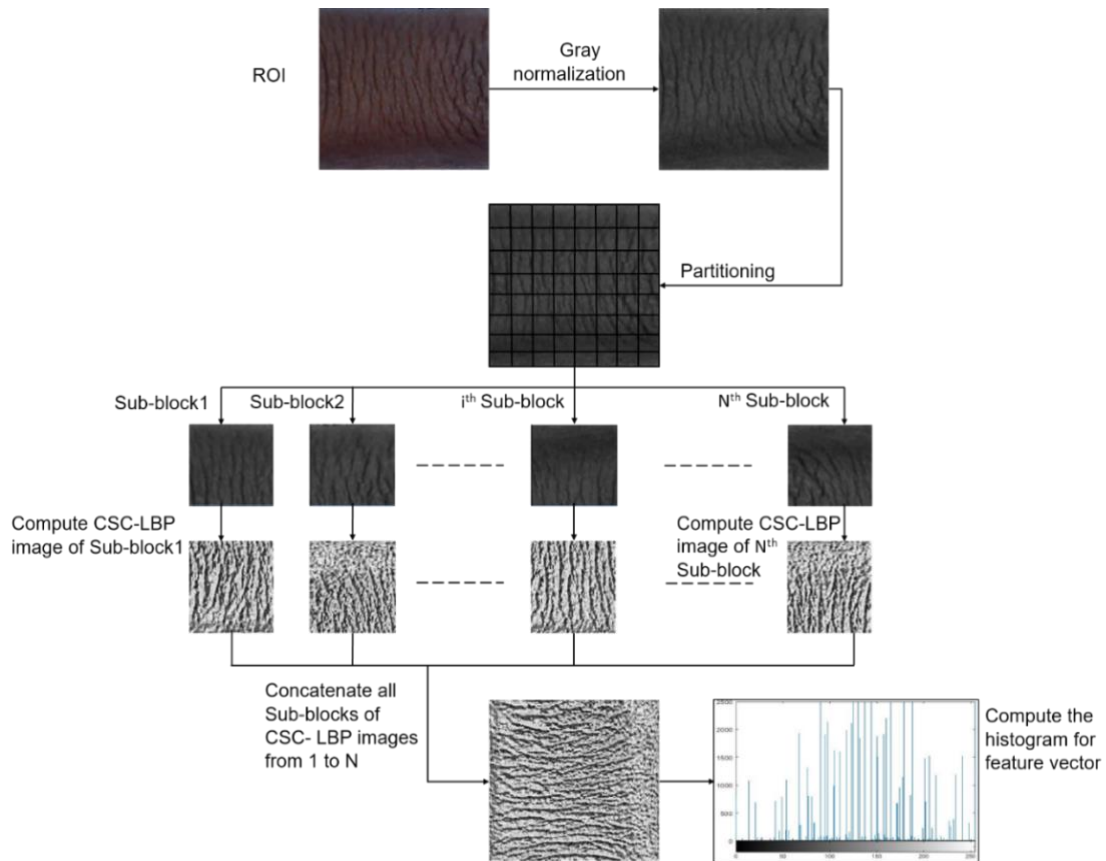


Figure 5. The MBCSC-LBP feature vector calculation

#### 4. RESULTS AND DISCUSSION

In this section, experiments with the self-collected dataset of dorsal finger creases are presented where support vector machine (SVM) with linear kernel is employed for classification purpose. The SVM is a supervised machine learning classifier which is primarily based on defining the optimal separating hyperplanes. The support vectors are points closest to the hyperplane, which play a critical role in defining the margin and hyperplane. Linear kernel is most widely utilized in applications where data can be separated linearly. The dataset is divided into two disjoint subsets with a ratio 70:30 for training and testing respectively. The classification processes run 10 times, and the average of these 10 experiments is reported in the results. For each run, seven images are used for training and the remaining three images are used for the testing purpose randomly. First, we conducted experiments using different combinations of circular shift LBP. We selected the combination that outperformed all other CSCLBP combinations for subsequent experiments to analyze the impact of varying the number of partitions i.e. NP 1, 4, 8, 16, 32, 64, 128 on the

selected LBP feature vector. Secondly, we proceed to assess the effect of partitions (NP) on the classification accuracy of the existing LBPs including center symmetric local binary pattern (CS-LBP) [25] and uniform local binary pattern (U-LBP) [26], and compare the performance of our method with these LBPs. The discussion can be made in several sub-sections.

#### 4.1. Selection of circular shift combination LBP value

Based on the equations of CSC-LBP, we conducted experiments using different combinations of circular shift LBP. The results for both right and left fingers are presented in Table 1. Based on Table 1, it can be observed that the classification accuracy decreases as the combinations move from two points to three points. Specifically, when considering feature vectors of only two-point combinations, such as corner points (0, 2, 4, 6) or midpoints (1, 3, 5, 7), the classification accuracy is higher compared to the accuracy of three and four-point feature vectors. The CSC-LBP<sub>04</sub> combination in Table 1 outperforms all other combinations, with classification accuracies of 90.94% and 87.04% for the right and left index fingers, respectively.

Table 1. Experimental results of right and left index fingers with different combinations of CSC-LBP

Circular shift LBP Combinations	Right index finger				Left index finger			
	Precision	Recall	F1-Score	Accuracy	Precision	Recall	F1-Score	Accuracy
CSC-LBP <sub>0-7</sub>	79.10	79.96	79.53	81.16	78.56	80.50	79.51	76.30
CSC-LBP <sub>02</sub>	88.85	89.60	89.22	90.22	84.57	86.04	85.30	84.07
CSC-LBP <sub>04</sub>	<b>89.43</b>	<b>90.72</b>	<b>90.07</b>	<b>90.94</b>	<b>89.11</b>	<b>89.08</b>	<b>89.05</b>	<b>87.04</b>
CSC-LBP <sub>06</sub>	88.42	89.23	88.83	89.86	85.15	85.03	85.09	84.07
CSC-LBP <sub>24</sub>	88.97	89.95	89.46	90.58	87.04	87.64	87.34	85.19
CSC-LBP <sub>26</sub>	87.53	88.90	88.21	89.13	87.97	88.16	88.34	85.19
CSC-LBP <sub>46</sub>	87.99	89.54	88.76	89.86	84.91	86.81	85.85	84.07
CSC-LBP <sub>024</sub>	80.92	82.74	81.82	82.97	77.20	77.52	77.36	75.93
CSC-LBP <sub>026</sub>	77.51	80.92	79.18	79.21	79.28	81.08	80.17	77.41
CSC-LBP <sub>046</sub>	81.98	82.57	82.28	83.33	77.85	78.87	78.36	76.67
CSC-LBP <sub>246</sub>	82.47	84.85	83.64	83.33	78.72	80.71	79.70	76.30
CSC-LBP <sub>0246</sub>	82.45	83.97	83.20	83.70	85.17	85.39	85.61	82.22
CSC-LBP <sub>13</sub>	88.30	89.05	88.67	89.49	85.54	86.47	86.00	83.33
CSC-LBP <sub>15</sub>	88.63	90.31	89.46	89.86	85.92	86.55	86.23	84.44
CSC-LBP <sub>17</sub>	87.84	89.82	88.82	90.22	83.85	84.44	84.15	82.59
CSC-LBP <sub>35</sub>	88.90	89.80	89.35	90.22	84.59	85.99	85.29	83.33
CSC-LBP <sub>37</sub>	85.18	86.67	85.92	86.96	84.72	85.89	85.30	82.22
CSC-LBP <sub>57</sub>	89.98	91.31	90.64	90.58	85.59	86.65	86.12	84.81
CSC-LBP <sub>135</sub>	81.23	82.94	82.07	83.33	76.57	78.67	77.61	75.19
CSC-LBP <sub>137</sub>	80.73	82.48	81.60	82.61	77.80	79.76	78.76	75.93
CSC-LBP <sub>157</sub>	77.10	79.32	78.19	79.21	78.20	80.28	79.23	77.04
CSC-LBP <sub>357</sub>	80.42	81.31	80.86	82.25	76.65	79.72	78.16	74.81
CSC-LBP <sub>1357</sub>	81.08	82.73	81.90	82.61	83.84	84.17	84.49	80.37

#### 4.2. Impact of block size on classification performance

In this section, we investigate the effect of different numbers of partitions on our proposed method. For the sampling radius 'one', the neighboring sampling points set to 8 and experiments are conducted for different NP to find the most suitable number of partitions with the highest classification accuracy. Table 2 illustrates the performance evaluation of right and left index fingers under various number of partitions. From Table 2, it can be seen that classification performance increases with a different number of partitions as compared to the whole image with no partitions. The best classification accuracy is achieved when a number of partitions,  $N_P = 8$ . Moreover, accuracy is decreased with a further increase in the number of partitions, which is due to the fact that a larger number of partitions will create insufficient texture information, and fewer partitions will result in local noise.

Table 2. Performance comparison with the different number of partitions for MBCSC-LBP<sub>04</sub>

Finger	Performance Metrics	Number of Partitions ( $N_P$ )						
		1	4	8	16	32	64	128
Right-Index	Precision	89.11	94.91	<b>96.09</b>	95.9	94.84	94.87	61.17
	Recall	89.08	95.02	<b>95.82</b>	96.05	95.01	94.8	53.36
	F1-Score	89.05	94.96	<b>95.95</b>	95.97	94.92	94.83	56.99
	Accuracy	87.04	94.74	<b>96.22</b>	95.52	94.56	94.41	57.44
Left-Index	Precision	89.43	92.04	<b>93.66</b>	93.33	92.48	92.61	35.98
	Recall	90.72	92.09	<b>94.31</b>	93.59	92.9	92.65	26.16
	F1-Score	90.07	92.06	<b>93.98</b>	93.45	92.69	92.63	30.28
	Accuracy	90.94	91.59	<b>94.11</b>	93.41	92.07	92.04	29.81

### 4.3. Comparison with existing LBP operators

In this section, we examined the performance of our method by comparing it with the two other typical CS-LBP and ULBP methods used for biometric recognition systems. The precision, recall, F1-Score, and accuracy reflect the performance. Table 3 shows the impact of partitioning on classification performance for different LBP methods, and it is evident that the classification accuracy is significantly improved after partitioning as compared to the results illustrated before partitioning. In Table 3, the number of partitions i.e. NP=1 represent the results of whole image with no sub-blocks division. The results after partitioning show that the classification accuracy of each operator is increased by 6-10% for right index finger and 8% to 10% for left index finger. Even with the idea of partition, it is noticed that the classification accuracy is drastically reduced at a higher number of partitions i.e. NP=128. This is due to the fact that insufficient texture information is produced from a larger number of blocks, and it also causes local noise, which leads to lower classification accuracy. Our experiments on the self-collected dataset show that the best classification performance is achieved for both left and right index fingers when the number of partitions is 8. The comparison of classification accuracies for the proposed MBCSC-LBP descriptor with CS-LBP and U-LBP with different image partitioning size is illustrated in Figure 6 and Figure 7 for right and left index fingers respectively. Figures show that the proposed MBCSC-LBP descriptor outperformed the existing LBP descriptors. Furthermore, it can also be concluded that the approach of image partitioning into subblocks has also increased the classification accuracies compared with traditional LBPs.

Table 3. Comparison of classification performance of existing LBPs before and after partitioning

Finger	LBPs	Performance Metrics	Number of partitions (N <sub>p</sub> )						
			1	4	8	16	32	64	128
Right-Index	CSLBP	Precision	89.85	90.19	<b>90.51</b>	89.38	89.21	89.02	58.58
		Recall	90.76	90.57	<b>90.71</b>	90.09	89.78	88.51	50.71
		F1-Score	90.30	90.38	<b>90.61</b>	89.73	89.49	88.76	54.36
		Accuracy	89.41	89.59	<b>89.67</b>	88.96	87.96	87.04	54.04
	ULBP	Precision	76.06	93.36	<b>95.32</b>	94.87	94.37	94.32	61.69
		Recall	76.02	93.01	<b>95.59</b>	94.98	94.98	94.27	52.38
		F1-Score	76.04	93.18	<b>95.45</b>	94.92	94.68	94.29	56.65
		Accuracy	72.76	92.33	<b>95.19</b>	94.52	93.78	93.22	56.15
Left-Index	CSLBP	Precision	87.10	88.81	<b>91.64</b>	88.96	89.67	88.74	34.60
		Recall	87.79	89.69	<b>92.12</b>	89.51	89.25	91.50	25.65
		F1-Score	87.44	89.25	<b>91.88</b>	89.23	89.45	90.10	29.45
		Accuracy	86.96	88.70	<b>91.37</b>	88.74	88.48	88.15	29.26
	ULBP	Precision	72.44	92.12	<b>93.15</b>	92.78	92.65	94.46	35.58
		Recall	76.66	92.39	<b>93.70</b>	92.40	91.91	94.93	26.39
		F1-Score	74.49	92.25	<b>93.42</b>	92.59	92.28	94.69	30.29
		Accuracy	70.00	91.93	<b>92.67</b>	92.11	91.48	94.07	30.67

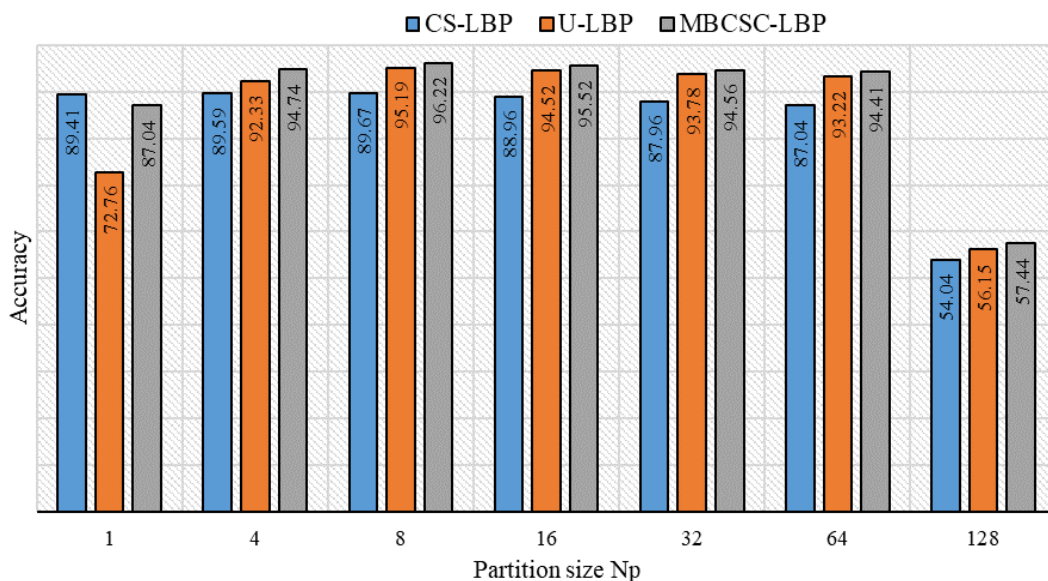


Figure 6. Accuracy comparison of different methods with varying partition size for the right index finger

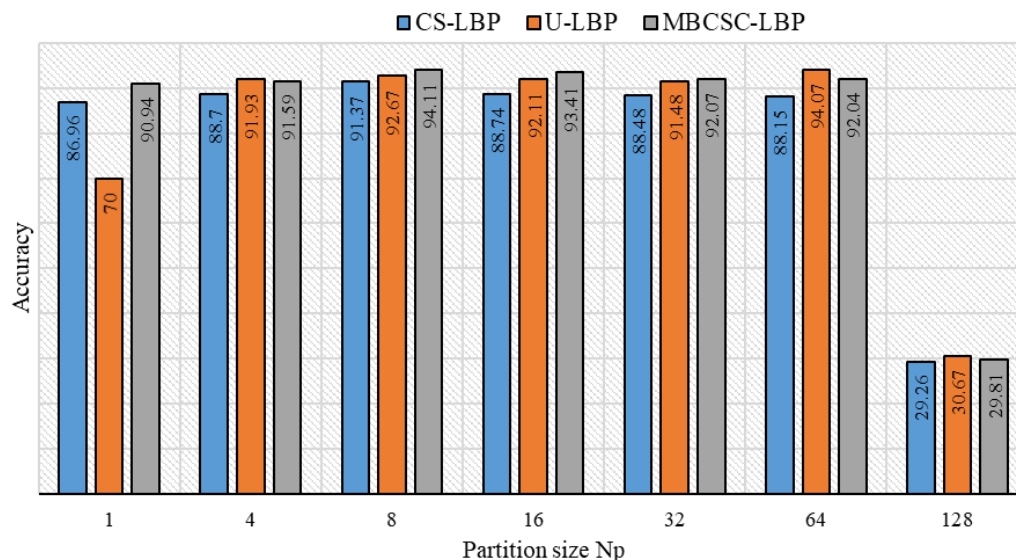


Figure 7. Accuracy comparison of different methods with varying partition size for the left index finger

## 5. CONCLUSION

The dorsal finger crease investigated in this paper contributes to develop a biometric recognition system with an alternate biometric modality, which provides a solution to the stakeholders for the users having risk of losing the fingerprints. Additionally, a MBCSC-LBP is proposed to extract the more discriminative features for dorsal finger crease. The impact of multi-block with local binary pattern features is evaluated for the dorsal finger crease classification system. The partitioning of DFC image into multi-blocks enhances the local and global image information, and minimizes the impact of noise to improve classification accuracy. Experiments were conducted on the DFC-USM database to verify the effectiveness of the proposed feature extraction algorithm. The experimental results revealed that the proposed approach with image partitioning enhances the classification performance by 8-10% as compared to the conventional circular shift combination-LBP, center symmetric-LBP and uniform-LBP. In the future, we aim to employ image partitioning with LBP features for other hand based biometric modalities using various LBP descriptors and classifiers for developing the multimodal biometric system.

## ACKNOWLEDGEMENTS

Acknowledgment to Ministry of Higher Education Malaysia for Fundamental Research Grant Scheme with project code: FRGS/1/2021/ICT02/USM/02/1 for the financial support of this research. The images used in this study are acquired through approval ethical protocol with the study protocol code USM/JEPeM/21100657.

## REFERENCES




- [1] H. Heidari and A. Chalechale, "Biometric authentication using a deep learning approach based on different level fusion of finger knuckle print and fingernail," *Expert Systems with Applications*, vol. 191, no. November 2021, p. 116278, 2022, doi: 10.1016/j.eswa.2021.116278.
- [2] H. Ren, L. Sun, J. Guo, and C. Han, "A dataset and benchmark for multimodal biometric recognition based on fingerprint and finger vein," *IEEE Transactions on Information Forensics and Security*, vol. 17, pp. 2030–2043, 2022, doi: 10.1109/TIFS.2022.3175599.
- [3] Z. Zhang and M. Wang, "Multi-feature fusion partitioned local binary pattern method for finger vein recognition," *Signal, Image and Video Processing*, vol. 16, no. 4, pp. 1091–1099, 2022, doi: 10.1007/s11760-021-02058-2.
- [4] K. H. M. Cheng and A. Kumar, "Contactless Biometric Identification Using 3D Finger Knuckle Patterns," *IEEE Transactions on Pattern Analysis and Machine Intelligence*, vol. 42, no. 8, pp. 1868–1883, 2020, doi: 10.1109/TPAMI.2019.2904232.
- [5] S. Prabu, M. Lakshmanan, and V. N. Mohammed, "A multimodal authentication for biometric recognition system using intelligent hybrid fusion techniques," *Journal of Medical Systems*, vol. 43, no. 8, 2019, doi: 10.1007/s10916-019-1391-5.
- [6] J. Dai, J. Feng, and J. Zhou, "Robust and efficient ridge-based palmprint matching," *IEEE Transactions on Pattern Analysis and Machine Intelligence*, vol. 34, no. 8, pp. 1618–1632, 2012, doi: 10.1109/TPAMI.2011.237.
- [7] S. Karanwal and M. Diwakar, "OD-LBP: Orthogonal difference-local binary pattern for face recognition," *Digital Signal Processing*, vol. 110, p. 102948, 2021, doi: 10.1016/j.dsp.2020.102948.
- [8] N. Hu, H. Ma, and T. Zhan, "Finger vein biometric verification using block multi-scale uniform local binary pattern features and block two-directional two-dimension principal component analysis," *Optik*, vol. 208, no. September 2019, 2020, doi:






- 10.1016/j.ijleo.2019.163664.
- [9] B. Sree Vidya and E. Chandra, "Entropy based local binary pattern (ELBP) feature extraction technique of multimodal biometrics as defence mechanism for cloud storage," *Alexandria Engineering Journal*, vol. 58, no. 1, pp. 103–114, 2019, doi: 10.1016/j.aej.2018.12.008.
- [10] M. Turkoglu and D. Hanbay, "Leaf-based plant species recognition based on improved local binary pattern and extreme learning machine," *Physica A: Statistical Mechanics and its Applications*, vol. 527, p. 121297, 2019, doi: 10.1016/j.physa.2019.121297.
- [11] K. Kaplan, Y. Kaya, M. Kuncan, and H. M. Ertuğ, "Brain tumor classification using modified local binary patterns (LBP) feature extraction methods," *Medical Hypotheses*, vol. 139, no. March, 2020, doi: 10.1016/j.mehy.2020.109696.
- [12] A. U. Wild and P., "Comparing verification performance of kids and adults for fingerprint, palmprint, hand-geometry and digitprint biometrics," *2009 IEEE 3rd International Conference on Biometrics: Theory, Applications, and Systems, Washington, DC, USA, 2009*, pp. 1–6, doi: 10.1109/BTAS.2009.5339069.
- [13] A. Attia, S. Mazaa, Z. Akhtar, and Y. Chahir, "Deep learning-driven palmprint and finger knuckle pattern-based multimodal Person recognition system," *Multimedia Tools and Applications*, vol. 81, no. 8, pp. 10961–10980, Mar. 2022, doi: 10.1007/s11042-022-12384-3.
- [14] G. K. Sidiropoulos, P. Kiratsa, P. Chatzipetrou, and G. A. Papakostas, "Feature extraction for finger-vein-based identity recognition," *Journal of Imaging*, vol. 7, no. 5, 2021. doi: 10.3390/jimaging7050089.
- [15] A. Kumar and C. Ravikanth, "Personal authentication using finger knuckle surface," *IEEE Transactions on Information Forensics and Security*, vol. 4, no. 1, pp. 98–110, 2009, doi: 10.1109/TIFS.2008.2011089.
- [16] A. Petpon and S. Srisuk, "Face recognition with local line binary pattern," *Proceedings of the 5th International Conference on Image and Graphics, ICIG 2009*, no. May, pp. 533–539, 2009, doi: 10.1109/ICIG.2009.123.
- [17] B. A. Rosdi, C. W. Shing, and S. A. Suandi, "Finger vein recognition using local line binary pattern," *Sensors*, vol. 11, no. 12, pp. 11357–11371, 2011, doi: 10.3390/s111211357.
- [18] L. Zhang, L. Zhang, and D. Zhang, "Finger-knuckle-print: A new biometric identifier," in *International Conference on Image Processing*, 2009, pp. 1981–1984. doi: 10.1109/ICIP.2009.5413734.
- [19] S. Yoon and A. K. Jain, "Longitudinal study of fingerprint recognition," *Proceedings of the National Academy of Sciences of the United States of America*, vol. 112, no. 28, pp. 8555–8560, 2015, doi: 10.1073/pnas.1410272112.
- [20] M. Drahansky, M. Dolezel, J. Urbanek, E. Brezinova, and T. H. Kim, "Influence of skin diseases on fingerprint recognition," *Journal of Biomedicine and Biotechnology*, vol. 2012, 2012, doi: 10.1155/2012/626148.
- [21] A. Uhl and P. Wild, "Experimental evidence of ageing in hand biometrics," *Proceedings of the 12th International Conference of the Biometrics Special Interest Group-(BIOSIG '13), Darmstadt, Germany, Sept. 2013*, pp. 39–50, 2013.
- [22] D. Kim and D. Yun, "A study on the effect of fingerprints in a wet system," *Scientific Reports*, vol. 9, no. 1, pp. 1–10, 2019, doi: 10.1038/s41598-019-51694-9.
- [23] I. Riaz, A. Nazri, and H. Ibrahim, "Circular shift combination local binary pattern (CSC-LBP) method for dorsal finger crease classification," *Journal of King Saud University - Computer and Information Sciences*, vol. 35, no. 8, p. 101667, 2023, doi: 10.1016/j.jksuci.2023.101667.
- [24] A. Kumar, "Importance of being unique from finger dorsal patterns: Exploring minor finger knuckle patterns in verifying human identities," *IEEE Transactions on Information Forensics and Security*, vol. 9, no. 8, pp. 1288–1298, 2014, doi: 10.1109/TIFS.2014.2328869.
- [25] M. Heikkilä, M. Pietikäinen, and C. Schmid, "Description of interest regions with local binary patterns," *Pattern Recognition*, vol. 42, no. 3, pp. 425–436, 2009, doi: 10.1016/j.patcog.2008.08.014.
- [26] T. Ojala, M. Pietikäinen, and T. Mäenpää, "Multiresolution gray-scale and rotation invariant texture classification with local binary patterns," *IEEE Transactions on Pattern Analysis and Machine Intelligence*, vol. 24, no. 7, pp. 971–987, 2002, doi: 10.1109/TPAMI.2002.1017623.

## BIOGRAPHIES OF AUTHORS






**Imran Riaz**    was born Kashmir, Pakistan in 1987. He received the B.Sc. degree in electrical engineering from the University of Azad Jammu and Kashmir, Pakistan, the M.Sc. degree in electronics engineering from Mirpur University of Science and Technology, (MUST), Mirpur Pakistan. He is doing PhD in computer vision and image processing at University Sains Malaysia (USM). His research interests include machine learning, computer vision, biometrics and image processing. He can be contacted at email [imran.ee@must.edu.pk](mailto:imran.ee@must.edu.pk).






**Ahmad Nazri Ali**    received the B.Eng., M.Sc., and Ph.D. degrees in electronics engineering from University Sains Malaysia. He is currently a senior lecturer with the school of electrical and electronics engineering, University Sains Malaysia (USM). As a researcher, he has several publications in reputed journals and also supervising master's and doctorate students. His research interests include embedded system, microprocessor and microcontroller applications, image processing and biometrics. He can be contacted at: [nazriali@usm.my](mailto:nazriali@usm.my).



**Haidi Ibrahim**    is (Senior Member, IEEE) and received the B.Eng. degree in electrical and electronic engineering from Universiti Sains Malaysia, Malaysia, and the Ph.D. degree in image processing from the center for vision, speech and signal processing (CVSSP), University of Surrey, U.K., in 2005. His research interests include digital image and signal processing, and analysis. He can be contacted at email: haidi@usm.my.



**Ilyas Ahmad Huqqani**    completed his BS and MS degrees in communication engineering at the Institute of Space Technology, Pakistan, in 2009 and 2013, respectively. His academic journey culminated in the successful acquisition of his PhD degree in computational intelligence and machine learning from the Universiti Sains Malaysia, Malaysia, in 2023. He has published numerous technical articles in refereed journals and conference proceedings. His current research interests encompass computational intelligence and machine learning. He can be contacted at email: ilyashuqqani@gmail.com.